Astron. Astrophys. 285, 393–403 (1994)

ASTRONOMY AND ASTROPHYSICS

# The quasar 3C395 revisited: new VLBI observations and numerical simulations

**L. Lara[1], A. Alberdi[1], J.M. Marcaide[1,2], and T.W.B. Muxlow[3]**

[1] Instituto de Astrofísica de Andalucía, CSIC, Apartado 3004, E-18080 Granada, Spain
[2] Universitat de València, E-46100 Burjassot, Valencia, Spain
[3] NRAL, Jodrell Bank, Macclesfield, Cheshire SK11 9DL, UK

Received 21 June / Accepted 20 November 1993

**Abstract.** We present the results of simultaneous VLBI observations of the quasar 3C395 at 2.3 and 8.4 GHz. Our maps show two well defined components (A and B) together with a weaker component in between (C2). The position of component C2 is compatible with the position of a component observed at epoch 1986.9 (component C1). We can interpret this positional coincidence *i)* assuming that component C2 and component C1 are just the same one, and hence C2 is stationary, or *ii)* considering that component C2 has travelled from the core to its current position, which now is coincident with the position of component C1 observed in 1986.9. The latter interpretation is supported by the total flux density evolution of 3C395. Based on this idea, we also present a model for 3C395 and numerical simulations of the time evolution of the emission of the compact structure at 2.3, 4.9 and 8.4 GHz which allow us to construct simulated maps of 3C395. The model and numerical simulations also provide a quantitative positional shift for the opaque core at 2.3 GHz with respect to 8.4 GHz which helps us to construct a spectral-index map of the source. Finally, our re-analysis of intermediate resolution VLBI observations at 0.6 GHz contribute to clarify the behavior of the jet beyond the cm-VLBI structure.

**Key words:** galaxies: jets – quasars: individual: 3C395 – techniques: interferometric – radio continuum: galaxies

## 1. Introduction

The radio source 3C395 (1901+319) is a 17th magnitude quasar with a redshift of $z = 0.635$ (Hewitt & Burbidge 1987). Radio observations at arcsecond scales show 3C395 as a compact unresolved core together with an extended component separated by 0.6 arcseconds in position angle P.A. $-57°$ measured north through east. Polarization observations made with the VLA at a frequency of 5 GHz (van Breugel et al. 1984) show that the extended component has a degree of polarization of 10% with the electric vector along P.A. 10°, while the compact component is 7.5% polarized with the electric vector along P.A. 70°. VLBI provides the necessary resolution to study the details of the core and shows it resolved in several sub-components (Phillips & Mutel 1980; Johnston et al. 1983; Phillips & Shaffer 1983; Waak et al. 1985; Simon et al. 1988a; Simon et al. 1988b). Two subcomponents have not changed their relative angular separation for 15 years, while a third has been observed moving superluminally between the previous two stationary components. This situation is reminiscent of that found in the compact structure of the quasar 4C39.25 (Alberdi et al. 1993). On the other hand, unlike 4C39.25, the VLBI structure of 3C395 is directed in a position angle almost opposite to that of the extended structure. Intermediate resolution observations (Saikia et al. 1990) suggest a sharp bending, possibly due to projection effects, of the VLBI jet towards the extended structure. Such sharp projected bends are unusual in extragalactic radio sources.

In this paper we present the results obtained from VLBI observations carried out on November 1st 1990 at 2.3 and 8.4 GHz simultaneously. These observations have led to the first high dynamic range VLBI map of 3C395 at 2.3 GHz and to the first VLBI map at 8.4 GHz. We have also carried out numerical simulations based on a relativistic jet model (Blandford & Königl 1979). With our simulations we intend to reproduce the compact structure in order to obtain the basic physical parameters which are determining the synchrotron emission, and understand the origin of the different jet components. These simulations also provide an approximate method for constructing a spectral-index map of the source by comparing the position of the peak of brightness of the core in our simulated maps at 2.3 and 8.4 GHz and shifting the observed maps according to the model displacement of the core. We have also re-analyzed previously published VLBI data of intermediate resolution at 0.6 GHz. The new maps help us to understand the behavior of the jet of 3C395 beyond the structure seen with cm-VLBI.

*Send offprint requests to*: L. Lara

**Table 1.** Calibration parameters

| Station | Diameter (m) | $T_{sys}$ (K) | Gain (K/Jy) | Freq. (GHz) |
|---|---|---|---|---|
| Effelsberg (Germany) | 100 | 60 | 1.28 | 8.4 |
| Medicina (Italy) | 32 | 105 | 0.10 | 2.3 |
| | | 110 | 0.15 | 8.4 |
| Noto (Italy) | 32 | 130 | 0.09 | 2.3 |
| | | 180 | 0.09 | 8.4 |
| Onsala (Sweden) | 20 | 78 | 0.03 | 2.3 |
| | | 105 | 0.05 | 8.4 |
| DSS65 (Spain) | 34 | 45 | 0.17 | 2.3 |
| | | 25 | 0.23 | 8.4 |
| Haystack (MA, USA) | 37 | 225 | 0.03 | 2.3 |
| | | 155 | 0.15 | 8.4 |
| OVRO (CA, USA) | 40 | 145 | 0.21 | 2.3 |
| | | 142 | 0.15 | 8.4 |
| VLA (NM, USA) | 26 × 25 | 26 | 1.4 | 8.4 |

## 2. Observations

On November 1st 1990 we observed the quasar 3C395 simultaneously at 2.3 and 8.4 GHz in right circular polarization (RCP). The following nine stations observed coordinated by the American and European networks: Effelsberg, Medicina, Noto, Onsala, DSS65, Haystack, phased VLA, OVRO and the VLBA antenna in Pie Town (see Table 1 for antenna characteristics). The average observation time with each antenna was $\sim$ 10 hours except for DSS65, where we only had 1.2 hours. We made observations of the quasar 3C395 phase-referenced to the core of the radio-galaxy 3C382 switching between the sources following a suitable duty cycle of 9 minutes. The stations used the Mark III recording system (Rogers et al. 1983), with a synthesized bandwidth of 56 MHz (Mode A), except for VLBA-PT which used a VLBA terminal and recorded a Mark III-compatible synthesized bandwidth of 32 MHz. The total bandwidth was split in two halves, allowing 28 MHz (or 16 for VLBA-PT) for each frequency band. Effelsberg and VLA, which did not record at S-band, only used 28 MHz.

We carried out the correlation of the data at the Max-Planck-Institut für Radioastronomie (MPIfR) in Bonn, Germany. We inserted compact and strong radio-sources (4C39.25, OQ208, 1642+690, 3C345, BL-LAC) at the beginning, middle and end of the observations to serve as fringe finders and as calibrators for the proper correction of the fringe rate. The VLBA-PT, with a rather new operating system which caused frequent formatter and clock problems at the time of the observations, did not yield fringes. We finally exported the data in Caltech package format for mapping purposes (Pearson 1991) and in a format compatible with the program VLBI3 (Robertson 1975) for astrometric purposes. The astrometric results of this work will be considered elsewhere.

We used measured system temperatures and gain curves, or antenna temperatures, supplied by the individual antennas to obtain an *a priori* calibration of the data. Table 1 summarizes the main parameters of the calibration. Subsequently, we derived antenna-based calibration corrections in phase and amplitude by means of the self-calibration technique (Cornwell & Wilkinson 1981). From the examination of the fringe amplitude at (u,v) crossing points, we estimate that the systematic errors in the final calibration of both data sets are of the order of 5–10%. We have used VLBI hybrid mapping algorithms to obtain our final images. We have also performed fits to the data using gaussian models to obtain quantitative estimates of the flux densities, positions and sizes of the source components.

## 3. Observational results

### *3.1. Observational history*

During the last decade the quasar 3C395 has been observed at different epochs and/or frequencies using VLBI arrays. Observations at wavelengths of 50cm (Padrielli et al. 1991), 18cm (Phillips & Mutel 1980; Simon et al. 1988a), 13cm (Phillips & Shaffer 1983), and 6cm (Johnston et al. 1983; Waak et al. 1985; Simon et al. 1988a; Simon et al. 1988b) have contributed to the idea of a quasar with a compact structure which essentially consists of two stationary components, labelled A and B hereafter, separated by a distance of $\sim$15 mas along a position angle of 118°. Some of these observations also detected a knot, which we shall name C1 hereafter, moving superluminally from the westernmost component, A, towards the easternmost component, B. The time evolution, through the different observing epochs, of the position relative to component A and flux density of these components are listed in Table 2. There are two different analysis of the data from epoch 1979.93 at 6cm: while the original analysis by Johnston et al. is much more consistent with the total flux density of the source at the observing epoch (1.85 Jy), the re-analysis by Waak et al. resulted in a flux density of 0.42 Jy for the core of 3C395, and in a total flux density of 0.90 Jy for the VLBI structure. The undetected 0.95 Jy were attributed to the arcsecond scale structure (0.32 Jy) and to a possible low brightness emission of $\sim$0.5 Jy located at 20 mas from the core along a position angle of $\sim$ 50°, which has not been detected in any other map. Nevertheless, Johnston et al. give a value too high for the flux density of component B and do not detect any emerging component from the core, while Waak et al. detect component C1 for the first time at 1.2 mas from the core.

Component A has revealed itself to be a very active feature in 3C395: a strong variability in its flux density at 5 GHz has been observed between 1979.9 and 1986.9. This fact, together with its flat spectrum and the detection of a component possibly superluminally separating from it, has led to the identification of component A with the core of 3C395. Component B, southeast from the core, has kept its relative distance from the core constant since the very early observations. There are slight variations in the distance between A and B from one frequency to another which could be explained in terms of opacity changes with the observing frequency. Additionally, component B shows a steep spectrum in the range of frequencies spanned by the existing observations. Finally, component C1, the su-

**Table 2.** Evolution of 3C395

| Date | $\lambda$ (cm) | Component | Flux Density (Jy) | Distance (mas) | P.A. (deg.) | Reference |
|---|---|---|---|---|---|---|
| 1978.39 | 18 | A | 1.0 | 0 | 0 | 1 |
| | | B | 1.5 | $15.6 \pm 0.2$ | $118.5 \pm 0.5$ | |
| 1979.93 | 6 | A | 0.87 | 0 | 0 | 2 |
| | | B | 0.74 | 15.9 | 118 | |
| 1979.93 | 6 | A | 0.42 | 0 | 0 | 4 |
| | | B | 0.38 | 15.6 | 118 | |
| | | C1 | 0.09 | $1.2 \pm 0.3$ | 118 | |
| 1980.59 | 13 | A | $\sim$0.8 | 0 | 0 | 3 |
| | | B | $\sim$1.6 | $\sim$15 | $\sim$120 | |
| 1983.26 | 6 | A | 0.64 | 0 | 0 | 4 |
| | | B | 0.40 | 15.6 | 118 | |
| | | C1 | 0.12 | $3.7 \pm 0.8$ | 118 | |
| 1984.92 | 18 | A | 0.33 | 0 | 0 | 5 |
| | | B | 0.94 | $15.1 \pm 0.1$ | $118.6 \pm 0.5$ | |
| | | C1 | 0.3 | $3.6 \pm 0.2$ | $117.5 \pm 3.5$ | |
| 1985.41 | 6 | A | 1.1 | 0 | 0 | 5 |
| | | B | 0.44 | $15.7 \pm 0.3$ | $118.4 \pm 1.1$ | |
| | | C1 | 0.09 | $4.7 \pm 0.3$ | $119.7 \pm 3.7$ | |
| 1986.89 | 6 | A | 1.2 | 0 | 0 | 6 |
| | | B | — | $\sim$15.3 | — | |
| | | C1 | — | 4.8 | — | |

References: (1) Phillips & Mutel 1980; (2) Johnston et al 1983; (3) Phillips & Shaffer 1983; (4) Waak et al. 1985; (5) Simon et al. 1988a; (6) Simon et al. 1988b

perluminal knot in 3C395, shows some peculiarities, namely, it is placed between two stationary components and exhibits one of the highest velocities reported in the literature ($0.64 \pm 0.10$ mas/yr, equivalent to a velocity of $13 \pm 2c$ assuming $H_o = 100$ h Km s$^{-1}$ Mpc$^{-1}$ and $q_o = 0.5$). Nevertheless, this superluminal motion does not seem to be uniform. The latter is especially critical if we consider the results from 1985.4 and 1986.9 (Simon et al. 1988b). From these two epochs an apparent proper motion of 0.08 mas/yr can be derived for component C1, which is incompatible with the apparent proper motion previously reported by Simon et al. (1988a).

### *3.2. Maps at 2.3 and 8.4 GHz*

In Fig. 1a-b we present hybrid maps of 3C395 made at 2.3 and 8.4 GHz. We have found no evidence of the extended arcsecond scale emission, which can be detected with the VLA or MERLIN, since our VLBI array resolves it completely. We can easily identify components A and B in Fig. 1. Nevertheless we consider that the identification of component C1 is not straightforward, due mainly to undersampling caused by the long period of time that has elapsed since the last VLBI observations of 3C395 (epoch 1986.9). Thus, an erroneous identification of this component and consequently a wrong proper motion measurement is possible. An additional difficulty for the identification of component C1 in our maps comes from the fact that this component was previously observed at 1.7 and 5 GHz but not at 2.3 or 8.4 GHz.

At 2.3 GHz, component A appears almost unresolved, with a particularly abrupt decrease in its flux density towards the west. Component B, placed from the core at a distance of 15.3 mas, similar to that of previous observations, appears resolved mainly towards the east. There is also a fainter, and almost resolved, emission to the east of component B that extends to the southeast direction and which can be still detected at about 24 mas from the core. Additionally, components A and B appear at 2.3 GHz connected by a continuous bridge of emission. This emission had not been detected in any previous VLBI image of 3C395 due to its steep spectrum, although there were some indications of it in the 5 GHz image of Simon et al. 1988a. Our map at 2.3 GHz also shows clearly an additional component between components A and B, which we shall name C2 in Fig. 1a.

The image shown in Fig. 1b is the first hybrid map of 3C395 ever made at 8.4 GHz. Component A, which we identify with the core, appears as a bright and unresolved component. There is a faint elongation, apparently emerging from A and directed southeast, which resembles the emission of a new component from the core. Nevertheless, several tests suggest that this structure could be the result of contamination of our clean map by the primary sidelobes of the interferometric beam. Component B is almost resolved out at 8.4 GHz, with a flux density much lower than at 2.3 GHz. In contrast to the 2.3 GHz map, there is no indication of emission between components A and B, except for a very weak component which we tentatively identify with component C2 on our 2.3 GHz map, and which appears close

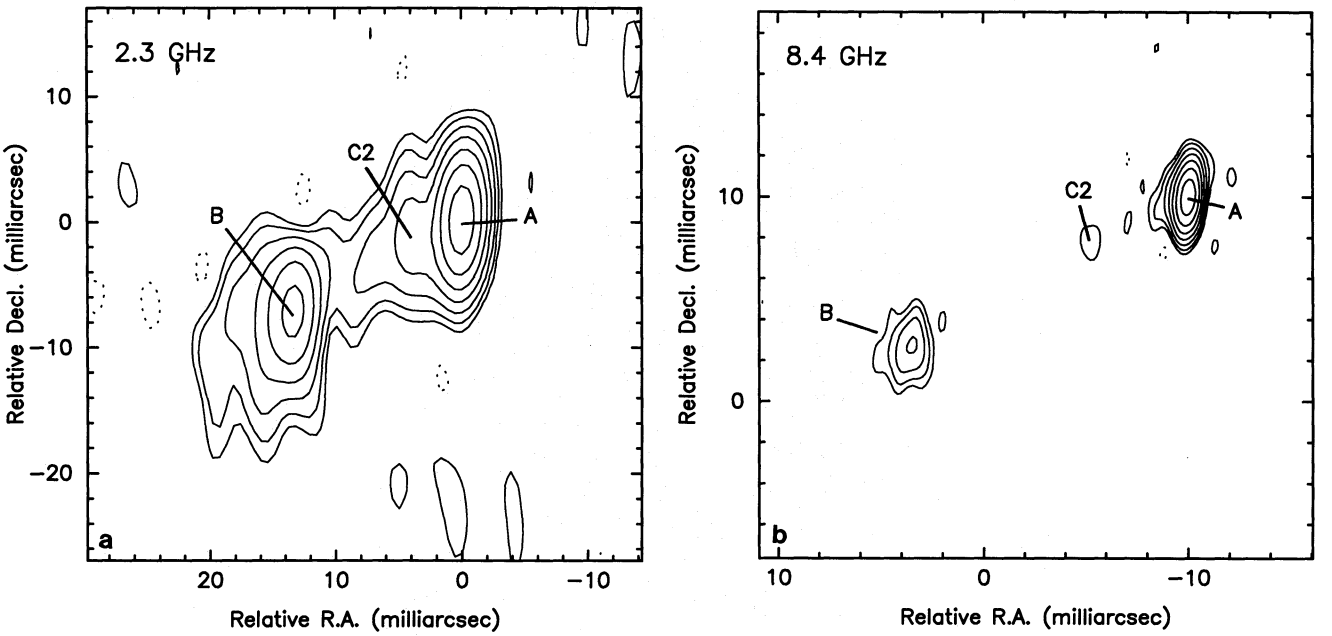


**Fig. 1a and b.** VLBI maps of 3C395 from epoch 1990.84. **a** Map at 2.3 GHz restored with a beam of 6.7 × 2.3 mas with the major axis along P.A. −2°. The peak brightness is 1.2 Jy/beam and the total map flux density 2.6 Jy. **b** Map at 8.4 GHz restored with a beam of 2.1 × 0.6 mas with the major axis along P.A. −2.2°. The peak brightness is 0.86 Jy/beam and the total map flux density 1.54 Jy. In both maps the contours represent -1,1,2,4,8,16,32, and 64% of the peak brightness

to the position observed in 1986.9 for the superluminal component C1. It is not clear whether this is pure coincidence or not. It is important for any interpretation of the structure of 3C395 to account for the strong deceleration suffered by component C1 between 1986 and 1987 and to explain the origin of the present component C2.

### *3.3. Map at 0.6 GHz*

In Fig. 2 we present a map made at 0.6 GHz, a result of a reanalysis of previously published data kindly provided by L. Padrielli. The observations date from June 1988 and correspond to a series of snapshots, each of approximately half an hour duration. (For a detailed description of the observations and analysis of the data see Padrielli et al. 1991). This map, which has been cleaned deeply in order to extract the low level emission, clearly shows a strong component corresponding to the now blended components A and B. It is possible to trace the jet beyond the compact structure seen in the higher frequency maps, and even to determine its curvature towards the arcsecond scale structure, supporting the interpretation of Saikia et al. (1990). It is remarkable that, in order to fit visibility data from the short baselines, we needed to consider the extended arcsecond scale structure.

### *3.4. Quantitative estimates*

To obtain quantitative estimates of the flux density, positions, and sizes of the components found at 2.3 and 8.4 GHz we have fitted simple elliptical gaussian models to the visibility data using a least-squares algorithm. A three component model provides the best fit to the visibility data at 2.3 and 8.4 GHz. The results of the fit are summarized in Table 3, where for both frequencies and for each component we display the flux density (S), the distance from the core (D), the position angle (P.A.), the length of the gaussian major axis (L), the ratio between the major and the minor axis (r) and the orientation of the major axis ($\phi$), defined in the same way as the position angle. The errors correspond to statistical standard errors. A question-mark means that the error is undetermined, probably because the parameter considered is not sufficiently well constrained by our data. From the flux density values in Table 3 we estimate the spectral indices of the components of 3C395 at the epoch of observation: $\alpha_A = -0.02 \pm 0.03$, $\alpha_B = -1.05 \pm 0.09$ and $\alpha_{C2} = -1.9 \pm 0.6$.

## 4. Discussion

### *4.1. The variability of the core of 3C395*

The compact core of 3C395 exhibits strong flux density variability at 5 GHz between 1980 and 1987 (see Table 2). In fact, the total flux density of 3C395 at the epochs of the VLBI observations shows an almost perfect correlation with the behavior of the core, indicating that the variations in the total flux density may be mainly explained through activity in the compact core region (Fig. 3).

A flux density monitoring program on 3C395 at 4.8, 8.0 and 14.5 GHz developed since 1980 (Aller et al. 1985 and Aller & Aller, private communication) reveals a remarkable increase in the total flux density since 1983 followed by a decrease be-

**Table 3.** Gaussian fit parameters

| Component | S (Jy) | D (mas) | P.A. (deg) | L (mas) | r | $\phi$ (deg) | Frequency (GHz) |
|---|---|---|---|---|---|---|---|
| A | 1.34±0.04 | 0 | 0 | 1.1±0.2 | 0.8±0.3 | 138±? | 2.3 |
| | 1.31±0.01 | 0 | 0 | 0.88±0.02 | 0.30±0.03 | 138±2 | 8.4 |
| B | 0.82±0.06 | 15.3±0.1 | 119.1±0.5 | 3.5±0.8 | 0.6±0.1 | 162±13 | 2.3 |
| | 0.21±0.01 | 15.5±0.1 | 118.5±0.2 | 1.9±0.3 | 0.6±0.1 | 148±10 | 8.4 |
| C2 | 0.24±0.06 | 4.6±0.6 | 111±8 | 3±1 | 0.3±? | 93±? | 2.3 |
| | 0.02±0.01 | 5.0±0.3 | 115±3 | 1.4±? | 0.4±? | 150±? | 8.4 |

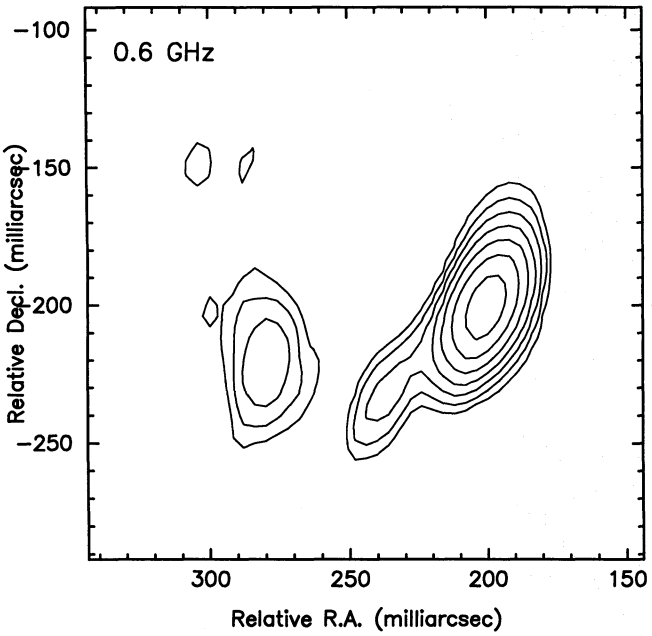


**Fig. 2.** VLBI map of 3C395 at 0.6 GHz from epoch 1988.4. This image has been convolved with an elliptical gaussian beam of 29 × 7 mas with the major axis along P.A. −17°. The contours represent -1,1,2,4,8,16,32, and 64% of the peak brightness of 0.86 Jy/beam. The total map flux density is 2.6 Jy

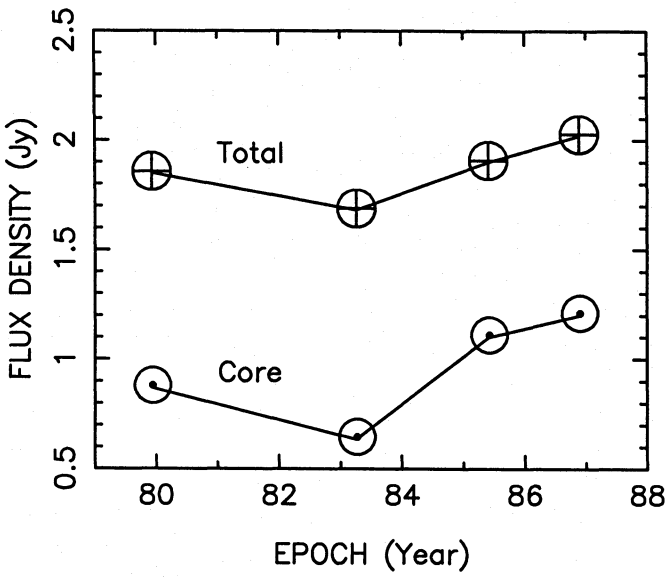


**Fig. 3.** Total and core flux density of 3C395 at the epochs of VLBI observations at 5 GHz. For epoch 1979.9 we have considered the core flux density given by Johnston et al.

tween 1987 and 1988. In view of this, and also considering that the ejection of new components from compact cores of radio sources may be correlated with events in the total flux density, it is very attractive to suggest that a new component may have been ejected from the core of 3C395 between 1983 and 1984. In fact, Valtaoja et al. (1988) found as a general result that the spectral shape and overall evolution of flux density flares fit well with a model where the flares result from shocks in an adiabatic, relativistic jet, as proposed by Marscher & Gear (1985). Such shocks would propagate along the jet and would be eventually detected as moving components. Finding or missing evidence of changes in the VLBI structure may be due more to observational limitations rather than to a sharp separation into transient flares and ejection of new knots. In 3C395, another increase in flux density observed since 1988 could indicate that we might be now in a situation similar to that of 1983–1984 and that a new component could be in the process of ejection. However, our 8.4 GHz observations were made at a suitable epoch to detect such a new component and we find no evidence for it. This can be explained if *i)* we hypothesize the existence of some unknown mechanism able to produce strong variability in the flux density of the core not directly associated to the ejection of components, and/or alternatively, *ii)* there is a delay between flaring and component ejection. Strong and unresolved bends merged within component A in 3C395 could provide suitable mechanisms to produce such retardation. In fact, bends in the vicinities of cores are a common phenomenon in compact radio sources, frequently observed with mm-VLBI (Krichbaum et al. 1993).

The existence of bends in the proximity of the core of 3C395 is partially suggested from the elongation along $\phi \sim 140°$ of the gaussian component which characterizes the core, which differs significantly from the position angle of components C1, C2 and B.

### 4.2. Stationary component B

Considering the position of component B measured at different epochs and frequencies, we have obtained, by means of a least-squares fit, a limit to its motion relative to the core of $-0.02 \pm 0.02$ mas/yr (see Fig. 4). Thus, we confirm the stationary nature of this component. Saikia et al. (1990) suggested that component B, at an angular separation of $\sim$ 15 mas from the core, is the inflection point of the jet towards the arcsecond scale structure seen with smaller interferometric arrays. However, our map at 0.6 GHz reveals that the jet extends much further out, $\sim$50 mas, in a position angle close to 130°, and then bends towards the north. We interpret component B to be the result of a bend in the relativistic jet towards the observer's line of sight which does not produce a significant variation in the observed position angle of the jet. The stationary nature of component B is then explained in terms of the curvature of the jet at a fixed position. The slight variations in the position of component B relative to the core could be mainly attributed to displacements of the peak of brightness of the core. Indeed, the small decrease in the distance of component B to the core reported by Simon et al. (1988b) is probably caused by the same reason which caused the deceleration of component C1.

Stationary components have been observed in other radio-sources, as for example 4C39.25 (Alberdi et al. 1993) or 1803+78 (Schalinski et al. 1992). The interpretation of such components as caused by bends of the jet towards the observer's line of sight underlines the lack of a need to classify these sources as a special class of AGN.

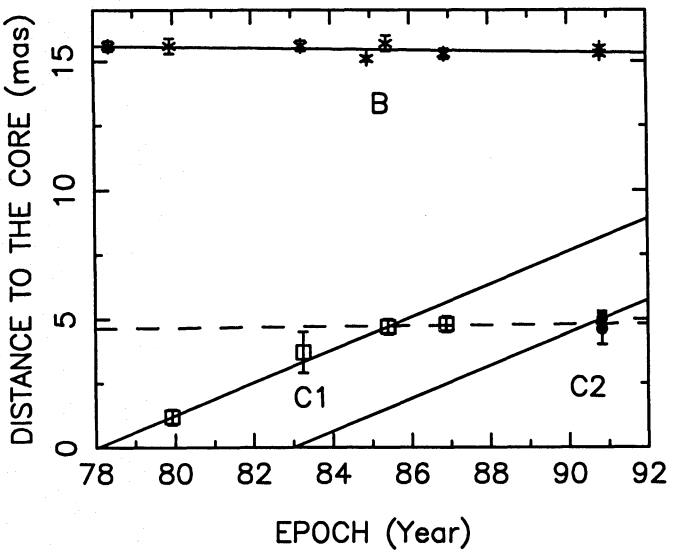


**Fig. 4.** Time evolution of the position of the components observed in 3C395 with respect to the core. Component B (*) has remained stationary since 1978. Component C1 (□) shows a peculiar behavior with superluminal motion (solid line) followed by a sharp deceleration in epoch 1986. The extrapolated zero-spacing epoch for this component is $\sim$ 1978. For component C2 (•) we plot two lines corresponding to the two possibilities presented in the text: *i)* the dashed line corresponds to the assumption that component C2 and component C1 in epochs 1985 and 1986 are the same one, and *ii)* the solid line assumes that C2 moves with the same apparent velocity as C1 (i.e. 0.64 mas/yr). The latter implies an extrapolated zero-spacing epoch around 1983

### 4.3. Superluminal motion in 3C395?

The maps presented in Fig. 1a-b represent the first high resolution images of 3C395 after a gap of four years. For superluminal radio sources this period of time makes it difficult to identify the different components within the structure observed at different epochs. If we consider component C2, its distance from the core derived from the modelfit is quite consistent with the distance of component C1 presented in 1986. This situation regarding component C2 is still unclear since it could be component C1 observed in 1986.9 or a new component that has travelled from the core to the current position during the time spanned between consecutive observations (see Fig. 4).

If we admit the first option, we must think about a plausible mechanism able to convert a superluminal component to a stationary one without any significant variation in its flux density, since the flux density of component C2 measured at 2.3 and 8.4 GHz is consistent with the flux density of component C1 at 5 GHz (see Table 2), as deduced from spectral index interpolation. Curvatures in the geometry of the jet, which would produce changes in the velocity of moving components, would also imply variability in the flux density due to the variation of the Doppler boosting factor. Other mechanisms, like interaction with a dense ambient medium capable of stopping a travelling component, is likely to be incompatible with the high stability of the jet, as seen in our 0.6 GHz map or in the 5 GHz map of Saikia et al. (1990). These difficulties, together with the lack of reported observations of stopping superluminal knots in other radio sources, make this idea implausible. However, also compatible with the identification of component C2 and component C1 in 1986.9 is the assumption that our component C2 is not related to a superluminal knot. In this case, a mechanism similar to the one which explains the stationary nature of component B would be appropriate to account for the lack of observed motion of component C2. A helical jet trajectory could describe this possible situation in 3C395, but it would not explain the apparent superluminal motion measured between 1979 and 1985.

Another valid explanation compatible with the experimental information acquired so far is our second option: If, as was suggested above, a new component was ejected around 1983–1984, then it could be tentatively associated with component C2. The possible date of ejection and the current distance from the core measured in our map at 8.4 GHz, $5.0 \pm 0.3$ mas, would imply an average superluminal velocity of $15 \pm 2c$, which is also compatible with the superluminal velocity previously reported for component C1 (Simon et al. 1988a).

Moreover, the ejection of a new component around 1983 could also be the reason, as suggested by Simon et al. (1988b), for the strong deceleration observed in component C1 between 1985.4 and 1986.9. Assuming that components C1 and C2 have the same proper motion of 0.64 mas/yr, we can estimate the flux density of component C2 at 5 GHz at epoch 1986.9 by

considering the flux density necessary to produce a shift in the peak of brightness of the unresolved "core-component C2" (flux density 1.2 Jy) sufficient to explain the apparent decrease in the velocity of component C1. Such calculations give a value of 0.5 Jy for component C2, and thus 0.7 Jy for the core. In its favour are the facts that these values are consistent with the flux density of the core in more quiescent epochs and the increase seen in the flux density curves by Aller et al. However, under these assumptions, the position of component C2 in 1986 should have been far enough from the core (1.85 mas) to be detected as an individual component with the array available in those observations. This would be in agreement with the existence of some kind of delay effect (bends in the jet?) in the ejection of components.

If component C2 is a new component, where is the old component C1? We know that as components move away from the core in other superluminal radio-sources, their flux densities decrease, mainly due to the quasi-adiabatic expansion of the jet. This may have occurred to component C1. Our map at 2.3 GHz shows faint emission eastward of component C2 at a distance of ~8 mas which could be tentatively associated with the old component C1. This distance would imply a superluminal velocity (0.6 mas/yr) compatible with the superluminal velocities reported in previous works.

Future VLBI observations will allow us to follow the evolution of component C2 and to select between the two presented options, namely, to identify component C2 with a stationary component, probably caused by a bend in the jet, or to consider components C1 and C2 as two different travelling knots which move superluminally along the jet.

## 5. Numerical simulations

We have used a numerical code (Gómez et al. 1993a) which computes the synchrotron emission from bent shocked relativistic jets in order to model 3C395. This code considers an input set of geometrical and physical parameters that can be iteratively improved to make the model emission match the observations. Our aim in the simulations, which we present here, is to provide a plausible and simple geometry for the jet and to explain the origin of the different jet components. Although we still do not have enough observational constraints to select between the two proposed models for component C2, in the simulations we have adopted the interpretation of two different shock waves, C1 and C2, travelling along the jet under the simplest assumptions for the geometry and the kinematics of the components. This interpretation is strongly suggested from the total flux density evolution of 3C395. Nevertheless, if component C2 is confirmed to be stationary, some modifications will have to be made to the geometry, and hence to the physical parameters used in these simulations. Thus, the derived numerical values of the different parameters must be understood as plausible, giving indication of the order of magnitude.

Considering the time evolution of the component C1, we can estimate the main geometrical parameters of the jet trajectory. The measured apparent superluminal velocity provides an upper limit to the deviation of the jet from the observer's line of sight, $\theta_{max} = 2\tan^{-1}\frac{1}{\beta_{app}}$. Since we do not have any measurement of the motion of component C2, we will assume that the new component travels with the same velocity as that reported for component C1, namely 0.64 mas/yr (≡ 13.2c). This superluminal velocity sets an upper limit of 8.7° to the angle to the observer. We will also assume that this velocity is constant, at least in those regions where moving components have been observed. In this region we will assume a straight jet at 8° from the observer's line of sight. Beaming effects and such a favorable orientation of the jet would prevent the detection of any milliarcsecond-scale counterjet in 3C395.

In order to simulate the stationary component B, we have assumed a bend in the jet towards the observer at a projected distance of ~15 mas. To reproduce the observed flux density of this component, the jet must reach a maximum orientation of 1° with respect to the observer. In this way, component B is simply the result of the magnification of the radiation due to Doppler boosting and its stationary character is guaranteed, as long as the bend corresponds to a fixed physical position. We have also assumed a narrow jet with a small opening angle, 0.2°; otherwise, adiabatic losses would prevent the formation of component B, placed far away from the core (~0.5 to 1 Kpc). The final geometry is shown in Fig. 5. For simplicity, we have not considered any bends on the projection plane of the sky, but just bends with respect to the observer's line of sight. The geometry in Fig. 5 is the simplest one capable of describing the general features of the observations.

Once the geometry is fixed, we iteratively determine the physical parameters that better reproduce the observed emission at different epochs and frequencies. To do that, we first simulate the quiescent jet without shock waves, to which we add the contribution from the different shock waves at different epochs. In this way, we reproduce the flux density at 2.3 GHz and 8.4 GHz , corresponding to epoch 1990.84 which we used as a reference for the quiescent jet, within discrepancies of 10% and 30%, respectively. Components C1 and C2 are interpreted as shock waves travelling along the jet, both with the same apparent velocity, $v_{app}$ = 13.2c. This velocity and the geometry correspond to $\beta$= 0.9992, or equivalently $\Gamma$ = 25, for both forward shock waves. To fully describe the shock waves, we have also assumed that they are 3 parsecs in length and that only 70% of the inner jet radius is shocked (Gómez et al. 1993b). Once we know the geometry and the velocity, we can determine the evolution of the shock waves along the jet, and thus obtain simulated maps at different epochs of observation. It is worth noting that the parameters which best describe the observations correspond to an optically thin core at 4.9 and 8.4 GHz; otherwise, we would have an inverted spectrum core, contrary to observations, and we would also have a large, and thus measureable, shift in the position of the peak of brightness of the core with the frequency. In order to reproduce the core flux density ratio between 2.3 and 8.4 GHz we have assumed that a new component was in the process of ejection in 1990, as suggested from the flux density curves of Aller & Aller (private commu-

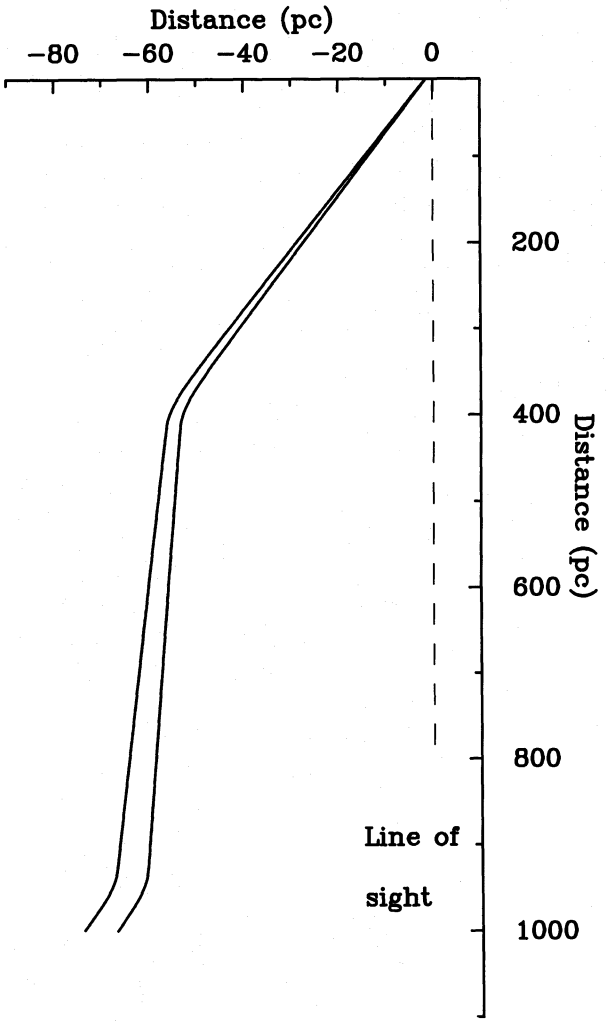


**Fig. 5.** Geometry of the jet of 3C395 used in the numerical simulations. Only the VLBI structure ($\sim$ 16 mas on the sky) is considered

nication). This component should not be resolved at any of the three frequencies we are considering.

The final set of parameters is displayed in Table 4. In Fig. 6 we present the simulated maps at different observing epochs between 1979 and 1990 at the frequencies of 2.3, 4.9 and 8.4 GHz.

The numerical simulations provide frequency dependent core positions as a result of changes in the optical depth (Marcaide & Shapiro 1984; Gómez et al. 1993a). Comparing the position of the peak of brightness of the core in our simulated maps at 2.3 and 8.4 GHz in 1990.84, we find that they differ by $\sim$ 0.7 mas. We can then shift both *observed* maps according to this model displacement and compute the spectral-index map of 3C395 between these two frequencies (see Fig. 7). Since we assume a straight jet in the vicinity of the core, we have performed the displacement of the maps along the jet predominant position angle, P.A. 118°. Additionally, in order to obtain a meaningful spectral-index map, the flux density maps must have the same resolution. Thus we have convolved both maps with the 2.3 GHz

**Table 4.** Jet physical parameters[a]

| | |
|---|---|
| Initial particle density per energy | $10^{-3}e^{-}cm^{-3}erg^{\gamma-1}$ |
| Minimum energy of electrons | 0.1 $erg$ |
| Total magnetic field, H | 1.35 $mGauss$ |
| Jet initial radius | 0.16 $pc$ |
| Electron energy spectral index | 2.2 |
| Jet flow velocity | 0.990 $c$ |
| Opening half angle | 0.18° |
| Fraction of randomly oriented field | 0.7 |
| Evolution of H with 1/r | 1.0 |
| Redshift of the quasar | 0.635 |
| Azimuth observer angle | 98° |

[a] As defined in Gómez et al. (1993a)

data beam. Finally, to minimize the contribution of noise in our intensity maps to the final spectral-index map, we have considered 1% as the limiting meaningful contour in our intensity maps.

Although this is a tentative method of constructing a spectral-index map (the accurate way would be by means of phase reference techniques, Marcaide & Shapiro 1984) we obtain a plausible map which shows a flat spectrum core followed by a steep spectrum jet. The differences in the spectral indices of components B and C2 (component B is flatter than C2) can be understood considering that the orientation of the jet towards the observer and the physical parameters involved are different. A favorable orientation of the jet produces an increase in the optical depth, which turns into a flattening of the spectrum.

There are features in the map, for example the positive contour in the southwest of component B, which are probably caused by artifacts of hybrid mapping or by the method of constructing the spectral-index map. We have estimated the uncertainty in the construction of our spectral-index map by introducing different shifts to the flux density maps around the previous shift of 0.7 mas. The spectral-index maps thus obtained show consistent results if the shifts are within $\pm$0.4 mas. Greater shifts produce implausible results, as for example, high values for the spectral indices in the western side of component B, or contours which are not normal to the axis of the brightness structure. Such a configuration of the contours was suggested as a useful criterion for making spectral-index maps by Marcaide & Shapiro (1984).

Although our modelled maps can be readily compared with the observations and reproduce the behaviour and spectral index of components A and B, there are some difficulties which cannot be overcome with our simple assumptions:

– There are serious discrepancies in the flux density levels at epochs different from 1990.84, which we used as a reference in the simulation of the quiescent jet. Assuming a straight jet in the vicinity of the core may be incorrect: possible bends in the jet would distort the motion of the shock waves, the time of ejection of the components from the core, and consequently, the total flux density evolution. Furthermore,

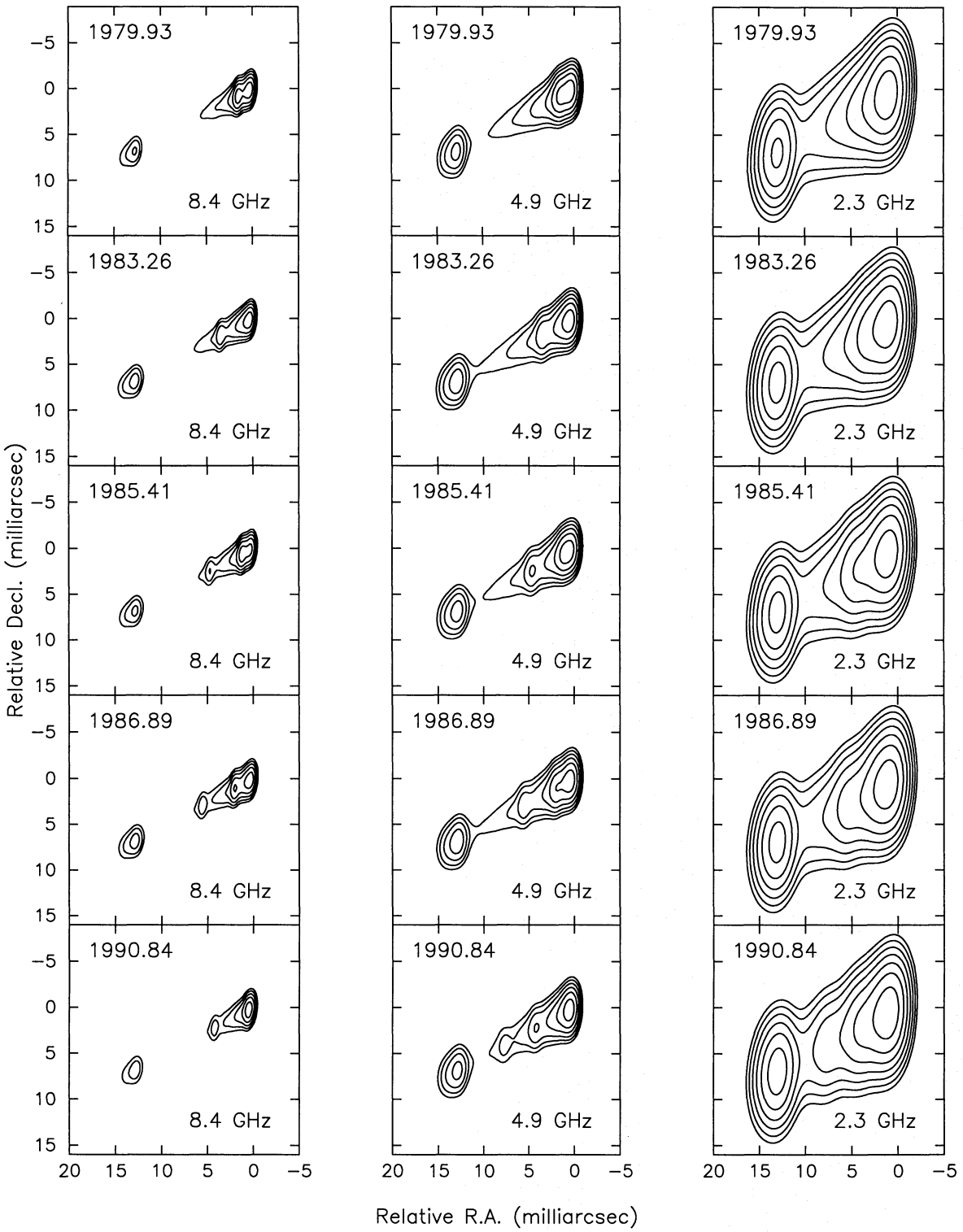


**Fig. 6.** Modelled maps of 3C395 obtained from numerical simulations. The 8.4 GHz maps are convolved with a beam of 2.1 × 0.6 mas with P.A. −4° and the contours represent 4,8,16,32, and 64% of the peak brightness of 0.46 (1979.9), 0.46 (1983.3), 0.56 (1985.5), 0.46 (1986.9) and 0.78 (1990.8) Jy/beam. The 4.9 GHz maps are convolved with a beam of 3 × 1 mas with P.A. −2° and the contours represent 1,2,4,8,16,32, and 64% of the peak brightness of 0.80, 0.79, 0.89, 0.79 and 0.98 Jy/beam for the corresponding epochs. The 2.3 GHz maps are convolved with a beam of 6.7 × 2.3 mas with P.A. −2° and the contours represent 1,2,4,8,16,32, and 64% of the peak brightness of 1.09, 1.06, 1.06, 1.09 and 1.04 Jy/beam for the corresponding epochs

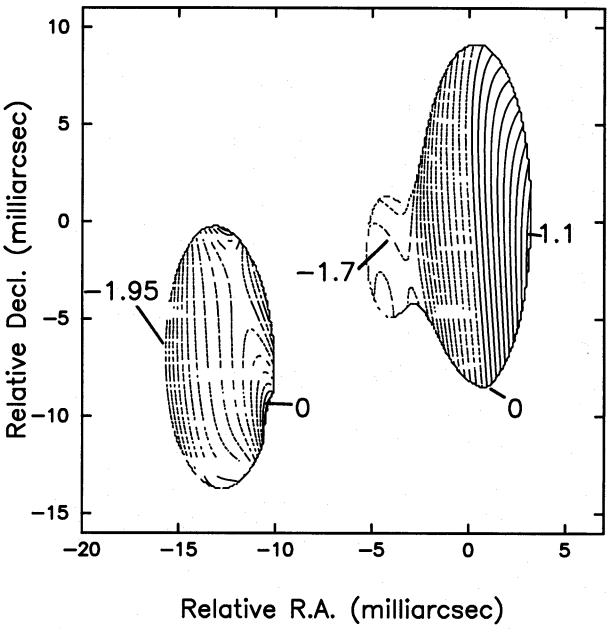


**Fig. 7.** Spectral-index map of 3C395 between 2.3 and 8.4 GHz corresponding to epoch 1990.84. Continuous lines indicate positive spectral indices ($\alpha \geq 0$, $S \propto \nu^{\alpha}$), and dashed lines, negative ones. The maximum, zero, and minimum values of the spectral index are indicated. Contour increment is $\Delta\alpha = 0.12$

we have not considered any kind of processes that would produce a time evolution of the physical parameters in Table 4 that we use in our simulations.

- We obtain too much emission between components A and B. This may be due to the simple geometry that we have assumed. Slight bends away from the observer's line of sight between these two components would produce a decrease in the emission, but on the other hand would complicate the geometry and the motion of the moving components. In addition, we cannot compare the dynamic range of real images with the "dynamic range" of simulations: while our simulated images contain all the flux density of the source, in real imaging we could be missing some low level emission.
- Our simulations show that in 1986.9, an inter-continental array should have clearly resolved from the core a component ejected in 1983–1984 moving with an apparent velocity of 0.64 mas/yr. Nevertheless, this component was not detected, although the core was slightly resolved towards the southeast. Apart from the indetermination of the velocity of component C2, we have assumed a constant velocity for the shock wave, even at jet regions giving rise to the core emission. Bends, again, would change this assumption, producing significant variations in the date of ejection, and thus in the results of our simulations.

## 6. Conclusions

We have observed the radio source 3C395 simultaneously at 2.3 and 8.4 GHz using VLBI techniques and have obtained new maps, which contribute to understand the compact structure and kinematics of 3C395 after a period of four years without high resolution information from this radio source. The maps that we have presented *i)* confirm component B as stationary with respect to the core component A, *ii)* show a component, C2, between component A and component B, whose identification as a moving component or as a result of a bend in the jet is still unclear, and *iii)* show a continuous bridge of emission at 2.3 GHz between components A and B.

On the basis of simple assumptions, we have made numerical simulations of the compact structure of 3C395 based on the computation of the synchrotron emission from bent shocked relativistic jets. We have found a geometry and a set of physical parameters which reproduce the general features of the observations. We have assumed a straight jet in the region where moving components have been observed, and a sharp bend towards the observer's line of sight which explains component B. Looking for a scenario compatible with previous observations and with the evolution of the total flux density of 3C395, we have assumed the existence of two travelling shock waves: the first, associated to component C1, detected and monitored in observations previous to 1987, and the second, associated to component C2, tentatively detected by us and presented in this work. However, we do not rule out the possibility of component C2 as the result of a bend in the jet. The identification of C2 as a new component is suggested by the time evolution of the total flux density. However, further observations are required to confirm its existence. In our simulations we have characterized both shock waves with the same parameters and have obtained simulated intensity maps that can be compared with the observations. The discrepancies between observations and simulations strongly suggest the existence of bends in the vicinity of the core. Highly sensitive observations at higher frequencies are needed to test the existence of such bends. Such observations would provide a deeper sight of the active nucleus of 3C395.

As an additional result derived from our numerical simulations, we have obtained a displacement of 0.7 mas in the position of the peak of brightness of the core at 2.3 with respect to 8.4 GHz. We have then taken advantage of such modelling result and of simultaneous observations at two different frequencies to construct a spectral-index map of the source, which is consistent with a flat core and steep spectrum jet.

Furthermore, we have shown that the inflection point towards the arcsecond scale structure is not associated with the stationary component B but rather is located at a distance of $\sim$ 70 mas from the core.

*Acknowledgements.* We wish to thank the EVN and US VLBI networks, and the staff of the different observatories for their contribution to the observations, and the MPIfR staff at the correlator for their efforts during the correlation. We also wish to acknowledge L. Padrielli for kindly offering her VLBI data, and H. Aller & M. Aller for providing their results prior to publication. We are especially indebted to J.L. Gómez for the discussion and valuable help provided during the simulation part of this research. We thank an anonymous referee for helpful comments during revision of this manuscript. This work has been partially supported by the Spanish DGICYT grant PB89-0009.

## References

Alberdi, A., Marcaide, J.M., Marscher, A.P. et al., 1993, ApJ, 402, 160
Aller, H.G., Aller, M.F., Latimer, G.E. et al., 1985, ApJS, 59, 513
Blandford, R.D., Königl, A., 1979, ApJ, 232, 34
Cornwell, T.J., Wilkinson, P.N., 1981, MNRAS, 196, 1067
Gómez, J.L. Alberdi, A., Marcaide, J.M., 1993a, A&A, 274, 55
Gómez, J.L. Alberdi, A., Marcaide, J.M., 1993b, in press.
Hewitt, A., Burbidge, G., 1987, ApJS, 63, 1
Johnston, K.J., Spencer, J.H., Witzel, A., Fomalont, E.B., 1983, ApJ, 265, L43
Krichbaum, T.P., Witzel, A.W., Graham, D.A., 1993. In: Jets in Extragalactic Radio Sources, H.J. Roeser & K. Meisenheimer (eds.), Springer, Heidelberg, p. 71
Marcaide, J.M. Shapiro, I.I., 1984, ApJ, 276, 56
Marscher, A.P., Gear, W.K., 1985, Ap.J., 298, 114
Padrielli, L., Eastman, W., Gregorini, L. et al., 1991, A&A, 249, 351
Pearson, T.J., 1991, BAAS, 23, 991
Phillips, R.B., Mutel, R.L., 1980, ApJ, 236, 89
Phillips, R.B., Shaffer, D.B., 1983, ApJ, 271, 32
Robertson, D.S., 1975, Ph.D. Thesis, Massachusetts Institute of Technology
Rogers, A.E.E., Capallo, R.J., Hinteregger, H.F., et al. 1983, Sci, 219,51
Saikia, D.J., Muxlow, T.W.B., Junor, W., 1990, MNRAS, 245, 503
Schalinski, C.J., Witzel, A., Krichbaum, T.P., et al. 1992. In: Workshop on Variability of Blazars, Valtaoja, E., Valtonen, M. (eds.), Cambridge University Press, p.225
Simon, R.S., Hall, J., Johnston, K.J. et al., 1988a, ApJ, 326, L5
Simon, R.S., Johnston, K.J., Spencer, J.H., 1988b. In: The Impact of VLBI on Astrophysics and Geophysics, IAU Symp. N.129, Reid, M.J., Moran J.M. (eds.), Kluwer Academic Publishers, p.21
Valtaoja, E., Haarala, S., Lehto, H., et al., 1988, A&A, 203, 1
van Breugel, W.J.M., Miley, G., Heckman, T., 1984, AJ, 89(1), 5
Waak, J.A., Spencer, J.H., Johnston, K.J., Simon, R.S., 1985, AJ, 90(10), 1989

This article was processed by the author using Springer-Verlag LaTeX A&A style file version 3.